

On collisions driven negative energy waves and Weibel instability of a relativistic electron beam in a quasi-neutral plasma

Anupam Karmakar¹, Naveen Kumar¹, Gennady Shvets², Oleg Polomarov², and Alexander Pukhov^{1*}

¹*Institut für Theoretische Physik I, Heinrich-Heine-Universität, Düsseldorf, 40225, Germany*

²*Department of Physics and Institute for Fusion Studies,*

University of Texas at Austin, One University Station, Austin, TX 78712, USA

A new quasi-neutral model describing the Weibel instability of a high-current relativistic beam propagating through a resistive plasma is developed. It treats beam electrons as kinetic particles, and ambient plasma as a non-relativistic fluid. For a finite-temperature beam, a new class of negative energy magneto-sound waves is identified, which can possess negative energy. Their growth due to collisional dissipation in the cold return current destabilizes the beam-plasma system even for high beam temperatures. We perform detailed two- and three-dimensional particle-in-cell (PIC) simulations of the thermal beam and collisional plasma. It is shown that in three dimensions, the Weibel instability persists even for physically collisionless background plasma. The anomalous plasma resistivity is then caused by the two-stream instability.

PACS numbers: 52.57.-z, 52.35.-g, 52.65.Rr

The fast ignition fusion (FI) is a promising route towards the laser driven fusion. In the classic FI scheme [1], a laser-generated relativistic electron beam with a few MeV per electron energy must propagate through overdense plasma to heat a hot spot in the core of a pre-compressed fusion fuel target. The current carried by these MeV electrons inside the plasma is much higher than the Alfvén current limit $I = (mc^3/e)\gamma = 17\gamma kA$, where m is the electron mass, e is the electronic charge, and γ is the Lorentz factor of the beam. Transportation of this electron beam is not possible unless it is compensated by a return plasma current. However, this configuration is unstable and the current beam is subject to the Weibel and the two-stream instabilities. The Weibel instability [2] is particularly responsible for the generation of very strong static magnetic fields (~ 100 MG) [3]. It is one of the leading instabilities under relativistic conditions and has been studied for a long time [4, 5, 6, 7, 8, 9, 10, 11, 12]. Honrubia *et al.* [11] have performed three-dimensional simulations of resistive beam filamentation corresponding to the full scale FI configuration. Three-dimensional magnetic structures generated due to the Weibel instability in a collisionless plasma have also been reported [12]. Recently, the evidence of Weibel-like dynamics and the resultant filamentation of electron beams have been reported experimentally [6]. It was proposed in Ref. [7] that this instability could be suppressed by the transverse beam temperature alone in a collisionless plasma. However, the instability persists in the presence of collisions in return plasma current no matter how high transverse beam temperature is. This regime of instability was termed as resistive beam instability [13].

In this Letter, we develop a theoretical approach to the collisional Weibel instability in the framework of the quasi-neutrality assumption. For a finite-temperature beam, a new class of negative energy magneto-sound

waves is identified. We derive conservation laws for the beam-plasma system and show that the energy of this system is not positively definite. Rather, it contains a negative term that allows for negative energy waves. Collisions in the background plasma current excite unstable magneto-sound waves in the system, which carry negative energy densities. Due to these waves the Weibel instability is not suppressed even when the transverse beam temperature would be high enough to stabilize collisionless plasma.

We present results of detailed 2D and 3D particle-in-cell (PIC) simulations on the relativistic electron beam transport in plasmas. The 2D geometry corresponds to a plane transverse to the beam propagation direction. In this geometry the Weibel instability is decoupled from the two-stream instability and we can study the effects of temperature and collisions on the Weibel instability systematically. The simulation results show that the Weibel instability cannot be suppressed by thermal effects alone if collisions are present in the system. We also make 3D PIC simulations of the Weibel instability. The simulation results show that in the full 3D geometry, the Weibel instability cannot be suppressed even in plasma free from binary collisions. We conjecture that the effective collisions leading to an anomalous resistivity in the return current are provided by the turbulence emerging from the electrostatic beam instability.

In the 2D simulations, we assume a very long electron beam propagating in the Z -direction and there is no dependence on the coordinate z . The beam and plasma densities are n_b and n_p respectively and the beam-plasma system is quasi-neutral *i.e.* $n_b + n_p = n_0$, where n_0 is the background ion density. Initially, the beam current is completely neutralized by the return plasma current. However, as the Weibel instability develops the current neutrality is destroyed due to the filamentation. The strongest magnetic field is generated in the transverse

plane ($x - y$ plane). This magnetic field generates an axial component of the electric field E_z . The transverse components of the electric field can be easily obtained from the force equilibration $\mathbf{E} + v_{pz} \times \mathbf{B}_\perp / c = 0$, where $v_{pz} = v_{pz} \mathbf{e}_z$ is the return current velocity. To summarize, these are the dominant electric and magnetic fields of the beam plasma system:

$$\mathbf{B}_\perp = -\mathbf{e}_z \times \nabla_\perp A_z, \quad E_z = -\frac{1}{c} \frac{\partial A_z}{\partial t}, \quad \mathbf{E}_\perp = -(v_{pz}/c) \nabla_\perp A_z, \quad (1)$$

where A_z is the z component of the vector potential. The B_z component is small, but can be approximated using $\partial_t B_z = -(\nabla_\perp v_{pz} \times \nabla_\perp A_z) \cdot \mathbf{e}_z$. The A_z component is determined from the Ampere law

$$\nabla_\perp^2 A_z = -\frac{4\pi}{c} (J_{bz} + J_{pz}), \quad (2)$$

where J_{bz} and J_{pz} are the current densities of the beam and plasma respectively. We discard the displacement current to ensure the quasi-neutrality. The axial equation of motion for the plasma flow and the transverse equations of motion for beam electrons are

$$\frac{\partial v_{pz}}{\partial t} + \nu v_{pz} = \frac{e}{mc} \frac{\partial A_z}{\partial t}, \quad (3)$$

$$\frac{d(\gamma_j v_{j\perp})}{dt} = -\frac{e(v_{jz} - v_{pz})}{mc} \nabla_\perp A_z, \quad (4)$$

where ν is the collisional frequency of the ambient plasma, m and c are the electron mass and velocity of light in vacuum respectively, and the subscript j represents the j^{th} beam electron. For collisionless plasma, Eq. (4) is written as

$$\frac{d(\gamma_j v_{j\perp})}{dt} = -\frac{e v_{jz}}{mc} \nabla_\perp A_z + \frac{e^2}{2m^2 c^2} \nabla_\perp A_z^2. \quad (5)$$

The second term in the RHS of Eq. (5) is due to the extra pinching of the electron beam by the transverse electric field \mathbf{E}_\perp . We note here that \mathbf{E}_\perp counters the magnetic expulsion of the ambient plasma. At the same time it reinforces magnetic pinching of the beam. The generalized momentum conservation in the z -direction gives

$$\gamma_j v_{jz} = \gamma_{j0} v_{jz0} + \frac{e}{mc} (A_z - A_{z0}). \quad (6)$$

If there is no dissipation, then we may derive conservation laws for the system. From Eqs. (2), (5) and (6), we have

$$\sum_j \gamma_j m c^2 - \sum_j \frac{m}{2} \left(\frac{e A_z}{mc} \right)^2 + \int d^2 x L_z \frac{|\nabla A_z|^2}{8\pi} + \int d^2 x L_z \frac{n_0 m}{2} \left(\frac{e A_z}{mc} \right)^2 = 0, \quad (7)$$

where L_z is the system length in the z direction. The first term in the above expression represents the total beam electron energy. The third and fourth terms correspond to the total magnetic energy and the plasma kinetic energy. The fourth term slightly overestimates the energy because the actual plasma density $n_p = n_0 - n_b$ is slightly smaller. The second term corrects this overcount: the excess energy is subtracted from the electron beam energy.

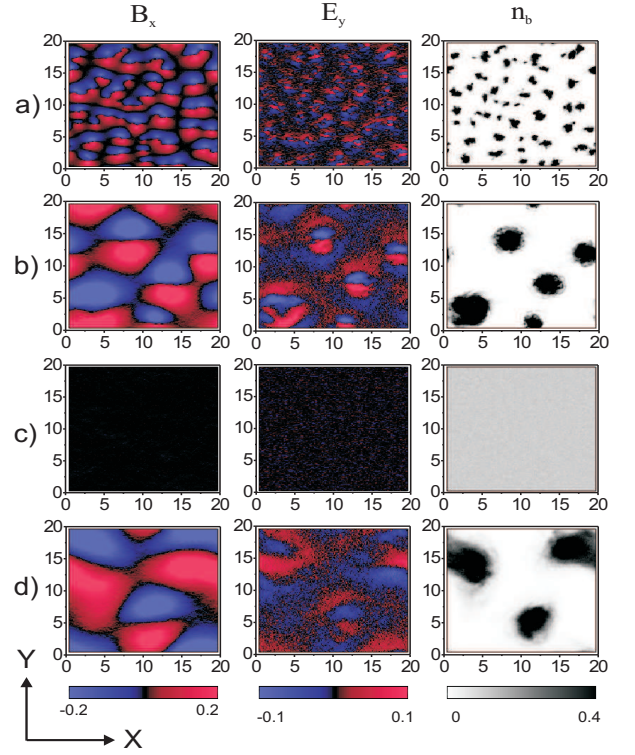


FIG. 1: (color online) Snapshots of the the evolution of transverse electromagnetic Weibel fields (E_x and B_x) and beam filament densities (n_b) during the nonlinear stage at a time $T = 20(2\pi/\omega_{pe})$ for four different simulation cases: (a) Cold electron beam in a collisionless background plasma, (b) cold e-beam in a collisional background plasma and (c) hot electron beam in a collisionless background plasma and (d) hot electron beam in a collisional background plasma.

The relativistic treatment of the instability could be somewhat cumbersome. However, the essential physics can be learnt from the non-relativistic equation of motion. For a warm electron beam the equation of motion reads as

$$m \frac{d\mathbf{v}_{b\perp}}{dt} = -e \frac{v_{bz} - v_{pz}}{c} \nabla_\perp A_z - \frac{\nabla_\perp P}{n_b}, \quad (8)$$

where P is the beam pressure related to the beam emittance. On linearizing Eq. (8) for small magnetic field perturbation, we have

$$\frac{d\delta\mathbf{v}_{b\perp}}{dt} = -c^2\beta_0\nabla_{\perp}\tilde{A}_z - 3\frac{v_{th}^2}{n_b}\nabla_{\perp}\delta n_b, \quad (9)$$

where $\tilde{A}_z = eA_z/mc^2$, $\beta_0 = (v_{bz} - v_{pz})/c \approx v_{bz}/c$, and it was assumed that $\nabla_{\perp}\delta P = 3v_{th}^2\nabla_{\perp}\delta n_b$. Eq. (9) together with the continuity equation $\partial_t\delta n_b = -n_b(\nabla_{\perp}\cdot\delta\mathbf{v}_{b\perp})$ yields

$$\left(\frac{\partial^2}{\partial t^2} - c_s^2\nabla_{\perp}^2\right)\frac{\delta n_b}{n_b} = c^2\beta_0\nabla_{\perp}^2\tilde{A}_z, \quad (10)$$

where $c_s^2 = 3v_{th}^2$ is the square of the beam's sound speed. Eqs. (2), (3), and (10) form a set of equations to describe the sound like perturbation/filamentation of the electron beam density. The simplest case of collisionless plasma ($\nu = 0$) and long wavelength perturbation ($|k_{\perp}| \ll \omega_p^2/c^2$, ω_p being the ambient plasma frequency) gives

$$\left(\frac{\partial^2}{\partial t^2} - \tilde{c}_s^2\nabla_{\perp}^2\right)\frac{\delta n_b}{n_b} = 0, \quad (11)$$

where $\tilde{c}_s^2 = c_s^2 - c^2\beta_0^2n_b/n_0$ is the modified sound speed. One may note that the cold beam ($c_s^2 < c^2\beta_0^2n_b/n_0$) is unstable due to the Weibel instability whereas the warm beam is stable. Under the warm beam approximation the dispersion for sound waves is given by $\omega^2 = \tilde{c}_s^2k_{\perp}^2$. These waves are stable and the Weibel instability does not occur for sufficiently high transverse beam temperature and low beam/plasma density ratios. With finite plasma resistivity taken into account the dispersion relation for the sound waves reads as

$$\omega^2 = \tilde{c}_s^2k_{\perp}^2 - \frac{\omega_b^2\beta_0^2k_{\perp}^2}{(k_{\perp}^2 + k_{pe}^2/(1 + i\nu/\omega))}. \quad (12)$$

where ω_b is the beam plasma frequency. For large scale perturbations ($k_{\perp}^2 \ll k_{pe}^2$, $k_{pe}^{-1} = c/\omega_p$) and small collision frequency, Eq. (12) yields two damped modes and one growing mode given by

$$\omega \approx \pm\tilde{c}_s k_{\perp} - i\nu\frac{c^2\beta_0^2n_b}{2\tilde{c}_s^2n_0}, \quad (13)$$

and

$$\omega \approx i\nu\frac{c^2\beta_0^2n_b}{\tilde{c}_s^2n_0}. \quad (14)$$

Thus collisions drive negative energy waves in the system, leading to the Weibel instability of a warm electron beam,

which would be stable in collisionless plasmas. This result has a profound impact on the understanding of the Weibel instability in plasmas.

To check our analytic theory, we carry out detailed 2D PIC simulations. The relativistic electron beam propagates in the negative \hat{z} -direction with the initial velocity $v_{b,z}$. The compensating return current of the ambient plasma electrons flows with the initial velocity v_p . The plasma ions are immobile and have the density $n_0 = n_b + n_p$. The simulation domain has the size $X \times Y = (20\lambda_s \times 20\lambda_s)$, where $\lambda_s = c/\omega_{pe}$ is the plasma skin length. All simulations are performed with 64 particles per cell and with a grid size of, $\delta x = \delta y = 0.125\lambda_s$. The density ratio between the beam and plasma electrons is $n_p/n_b = 9$, whereas the beam and background plasma electrons have velocities $v_b = 0.9c$ and $v_p = 0.1c$. The binary collisions are simulated with a newly implemented collision module in the relativistic PIC code Virtual Laser Plasma Laboratory (VLPL) [14]. We record the evolution of field energy for every component F_i of the fields \mathbf{E} and \mathbf{B} as $\int_S (eF_i m_e c \omega_{pe})^2 dx dy$ where $eF_i/m_e c \omega_{pe}$ represents the relativistic field normalization.

We use the electron beam initial temperature of $T_b \sim 70$ keV and the ambient plasma collision frequency $\nu_{ei}/\omega_p = 0.15$ for these simulations.

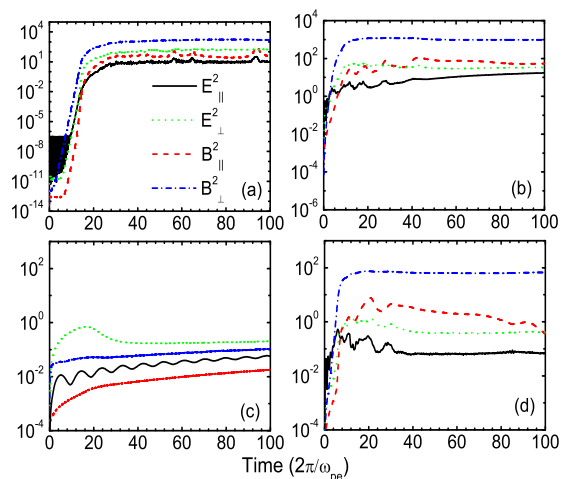


FIG. 2: (color online) Time evolution of the perpendicular and parallel Weibel \mathbf{E} \mathbf{B} field energies (E_{\perp}^2 , B_{\perp}^2 , E_{\parallel}^2 , B_{\parallel}^2) for four different simulation cases as described in the previous Fig. 1.

Fig. 1 shows snapshots of the transverse E and B fields, and the structure of the beam filaments at the time, $T = 20(2\pi/\omega_{pe})$ for four different cases: (a) cold electron beam and collisionless background plasma, (b) cold electron beam and collisional plasma (c) hot electron beam and collisionless plasma and (d) hot electron beam and collisional background plasma. The beam density fila-

mentation is shown in the last column in each panel. In collisionless case (a), the filaments are small, comparable with the background plasma electron skin depth. In the collisional case (b), the filament size is bigger. This can be explained as a collisional diffusion of plasma electrons across the self-generated magnetic fields. In the third panel of figure, simulation case (c), the electron beam is hot with the transverse temperature $T_b = 70$ keV, and the background plasma electrons are collisionless. Here we see no filament formation. The temperature of the electron beam stabilizes the Weibel instability. Physically the thermal pressure of the electron beam prevails over the magnetic pressure in this case. Hence, the magnetic field pinching which actually drives the instability does not occur resulting in the suppression of the Weibel instability. The last panel of the figure depicts the filament formation in the simulation case (d), where electron beam is hot and the plasma is collisional. Although the beam temperature is the same as in the stable collisionless case (c), the background plasma collisions revive back the instability. This is due to the collision induced generation of negative energy waves as discussed earlier in the theoretical model.

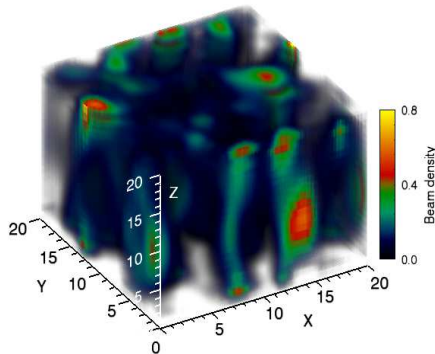


FIG. 3: (color online) Beam filaments from 3D PIC simulations. The ambient plasma is cold and collisionless, while the electron beam is hot and collisionless. The other parameters are same as in Fig. 1(c).

Fig. 2 shows the evolution of electric and magnetic field energies in the four cases corresponding to the simulations in Fig. 1. The energy axes in Fig. 2 use logarithmic scales. We see a stage of linear instability, where the field energies build up exponentially in time. It is followed by a nonlinear saturation. The linear instability stage is present in the simulations (a), (b) and (d). The simulation (c), where the electron beam had high temperature and the background plasma was collisionless, shows no linear instability and no significant build up of the magnetic field energy.

The linear growth rates calculated from the simulations results agree well with the theoretical model. After the linear stage of the instability, an electrostatic regime

of the filamentation instability characterized by the magnetic attraction of the filaments starts and the field energies saturate. Some small fluctuations around the saturated field energies can be seen. These fluctuations occur due to the collective merging of the filaments as also discussed in [9].

We also have done a number of 3D PIC simulations of Weibel instability, varying the beam temperature and the plasma collision frequency. To our surprise, we found no stabilization even in the collisionless case for high beam temperatures. The corresponding simulation is shown in Fig. 3. Although the electron beam in this simulation had the high transverse temperature, and the plasma had no binary collisions, we see a lot of filamentation due to the Weibel instability. We explain this fact in terms of anomalous plasma collisionality. Indeed, there is an oblique mode in the 3D geometry which couples the Weibel and the two-stream instabilities [8]. The two-stream mode generated electrostatic turbulence in the plasma. Stochastic fields associated with this turbulence scatter the beam and plasma electrons and lead to an effective collisionality in the return current. This anomalous effect revives back the Weibel instability. It may be noted here that we have always taken the background plasma as cold. The allowance of finite background plasma temperature decreases the growth rate of the instability. The interplay of collisions in different regimes of beam and background plasma temperatures can be found in Refs.[5].

In summary, we have developed a simplified model which identifies the collisional Weibel instability as the instability of the unstable negative energy mode driven by the collisions in the background plasma. An important result of this study is that beam temperature does not kill the Weibel instability in the presence of collisions in beam plasma system. An alternate explanation on the persistence of the Weibel instability in 3D geometry is offered. It is attributed to the anomalous collisionality of the beam-plasma system due to the two-stream mode. We have also derived the conservation laws for the beam plasma system which are useful for benchmarking the numerical codes. Detailed 2D simulations on the Weibel instability of an electron beam in two-dimensional transverse geometry have been performed, which essentially confirm the theoretical prediction.

This work was supported by the DFG through TR-18 project and the US Department of Energy grants DE-FG02-04ER41321 and DE-FG02-04ER54763.

* Electronic address: pukhov@tp1.uni-duesseldorf.de

- [1] M. Tabak *et al.*, Phys. Plasmas **1**, 1626, (1994).
- [2] E.S. Weibel, Phys. Rev. Lett. **2** 83, (1959).
- [3] A. Pukhov and J. Meyer-ter-Vehn, Phys. Rev. Lett. **76**, 3975 (1996), M. V. Medvedev and A. Loeb, ApJ **526**,

- 697, (1999).
- [4] R. Lee and M. Lampe, Phys. Rev. Lett. **31**, 1390 (1973), P. H. Yoon and R. C. Davidson, Phys. Rev. A **A35**, 2718, (1987), A. Pukhov and J. Meyer-ter-Vehn, Phys. Rev. Lett. **79**, 2686 (1997), F. Califano, F. Pegoraro and S. V. Bulanov, Phys. Rev. E **56**, 963 (1997), Y. Sentoku, K. Mima, S. Kojima and H. Ruhl, Phys. Plasmas **7**, 689 (2000), L. Gremmilet, G. Bonnaud and F. Amiranoff, Phys. Plasmas, **9**, 941 (2002), Y. Sentoku, K. Mima, P. Kaw and K. Nishikawa, Phys. Rev. Lett. **90**, 155001 (2003), J. M. Hill, M. H. Key, S. P. Hatchett, and R. R. Freeman, Phys. Plasmas **12**, 082304 (2005), O. Polomarov *et al.*, Phys. Plasmas **14**, 043103, (2007).
- [5] C. Duetsch, A. Bret, M. C. Firpo and P. Fromy, Phys. Rev. E **72**, 026402 (2005), J. M. Wallace, J. U. Brackbill, C. W. Cranfill, D. W. Forslund, and R. J. Mason, Phys. Fluids **30**, 1085 (1987), M. Honda, Phys. Rev. E **69**, 016401 (2004), T. Okada and K. Niu, J. Plasma Phys. **23**, 423 (1980), **24**, 483 (1980), W. Kruer, S. Wilks, B. Lasinski, B. Langdon, R. Town, and M. Tabak, Bull. Am. Phys. Soc. **48**, 81 (2003).
- [6] R. Jung *et al.*, Phys. Rev. Lett. **94**, 195001 (2005), M. Tatarakis *et al.* Phys. Rev. Lett. **90**, 175001 (2003), M. Wei *et al.* Phys. Rev. E **70**, 056412 (2004).
- [7] L. O. Silva, R. A. Fonseca, J. W. Tonge, W. B. Mori, and J. M. Dawson, Phys. Plasmas, **9**, 2458, (2002).
- [8] A. Bret, M.-C. Firpo and C. Deutsch, Phys. Rev. E **70**, 046401 (2004), Phys. Rev. Lett. **94**, 115002 (2005), Laser Part. Beams, **24**, 27 (2006), A. Bret, L. Grimmlet, D. Benisti and E. Lefebvre, Phys. Rev. Lett. **100**, 205008 (2008).
- [9] M. Honda, J. Meyer-ter-Vehn and A. Pukhov, Phys. Rev. Lett. **85**, 2128, (2000).
- [10] J. J. Honrubia, M. Kaluza, J. Schreiber, G. D, Tsakiris and J. Meyer-ter-Vehn, Phys. Plasmas, **12**, 052708 (2005), J. J. Honrubia, C. Alfonsen, L. Alonso, B. Perz and J. A. Cerrada, Laser Part. Beams, **24**, 217 (2006).
- [11] J. J. Honrubia and J. Meyer-ter-Vehn, Nucl. Fusion, **46**, L-25 (2006).
- [12] F. Califano, D. Del Sarto and F. Pegoraro, Phys. Rev. Lett. **96**, 105008 (2006)
- [13] K. Molvig, Phys. Rev. Lett. **35**, 1504 (1975).
- [14] A. Pukhov, J. Plasma Phys. **61**, 425, (1999).